Environmental Science & Technology

Article

Cite This: Environ. Sci. Technol. 2019, 53, 6738−6746

pubs.acs.org/est

Photochemical Transformations of Dichloroacetamide Safeners

Andrew E. Kral,[†,‡] Nicholas C. Pflug,[†,§] Monica E. McFadden,[‡] Gregory H. LeFevre,[‡,#] John D. Sivey,[∥] and David M. Cwiertny*[,‡,⊥,#,▽,○]

[‡]Department of Civil & Environmental Engineering, University of Iowa, 4105 Seamans Center for the Engineering Arts and Sciences, Iowa City, Iowa 52242, United States

[§]Department of Chemistry, University of Iowa, E331 Chemistry Building, Iowa City, Iowa 52242, United States

[∥]Department of Chemistry, Towson University, 543 Smith Hall, Towson, Maryland 21252, United States

[⊥]Department of Chemical & Biochemical Engineering, University of Iowa, 4133 Seamans Center for the Engineering Arts and Sciences, Iowa City Iowa 52242, United States

[#]IIHR—Hydroscience & Engineering University of Iowa, 100 C. Maxwell Stanley Hydraulics Laboratory, Iowa City, Iowa 52242, United States

[▽]Center for Health Effects of Environmental Contamination, University of Iowa, 251 North Capitol Street, Chemistry Building - Room W195, Iowa City, Iowa 52242, United States

[○]Public Policy Center, University of Iowa, 310 South Grand Avenue, 209 South Quadrangle, Iowa City, Iowa 52242, United States

Supporting Information

ABSTRACT: Dichloroacetamide safeners are commonly added to commercial chloroacetamide herbicide formulations and widely used worldwide, but their environmental fate has garnered little scrutiny as a result of their classification as "inert" ingredients. Here, we investigated the photolysis of dichloroacetamide safeners to better understand their persistence and the nature of their transformation products in surface waters. High-resolution mass spectrometry (HRMS) and nuclear magnetic resonance (NMR) spectroscopy were used to characterize photoproducts. Of the four commonly used dichloroacetamide safeners, only benoxacor undergoes direct photolysis under simulated natural sunlight ($t_{1/2}$ ∼ 10 min). Via a photoinitiated ring closure, benoxacor initially yields a monochlorinated intermediate that degrades over longer irradiation time scales to produce two fully dechlorinated diastereomers and a tautomer, which further photodegrade over several days to a structurally related aldehyde confirmed via NMR. Dichlormid, AD-67, and furilazole were more slowly degraded by indirect photolysis in the presence of the photosensitizers nitrate, nitrite, and humic acid. Reactive entities involved in these reactions are likely hydroxyl radical and singlet oxygen based on the use of selective quenchers. These safeners also directly photolyzed under higher energy ultraviolet (UV) light, suggesting their potential transformation in engineered systems using UV for disinfection. The finding that dichloroacetamide safeners can undergo photolysis in environmental systems over relevant time scales demonstrates the importance of evaluating the fate of this class of "inert" agrochemicals.

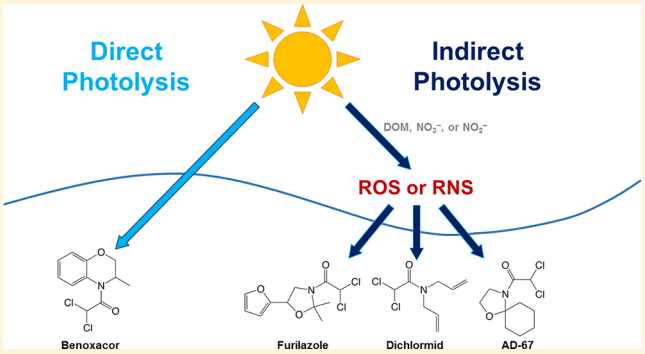

INTRODUCTION

A challenge with commercial herbicides is unintended toxicity toward crops.[1−5] One way to reduce such damage is through the addition of a chemical "safener",[2,3] which protects crops by boosting their biochemical response to herbicide exposure (e.g., increased expression of glutathione *S*-transferases).[6−8] Safeners are classified and regulated as "inert" ingredients because their use is not intended to mitigate weeds or other pests.[9,10] This classification has also brought less scrutiny of their environmental fate and effects; indeed, little environmental fate data are available, despite the heavy use of safeners in popular herbicide formulations.[11]

Dichloroacetamides are a commonly used class of safeners that can undergo transformations in the environment that could alter their bioactivity, including their non-target toxicity.[11,12] Dichloroacetamide safeners (Table S1 of the Supporting Information) are used to protect crops (e.g., corn, rice, and soybeans) from chloroacetamide herbicides, including acetochlor and metolachlor.[11] The difference in bioactivity of these two structurally similar classes of compounds stems in

Received: February 10, 2019
Revised: May 15, 2019
Accepted: May 18, 2019
Published: May 22, 2019

DOI: 10.1021/acs.est.9b00861
Environ. Sci. Technol. 2019, 53, 6738−6746

large part from their number of incorporated chlorine atoms; dichloroacetamide safeners possess two chlorine atoms bonded in a geminal relationship, whereas chloroacetamide herbicides contain only one chlorine atom. Notably, this structural similarity allows for the environmental transformation of inert safeners into structures similar (or, in one case, identical) to active herbicide ingredients through stepwise dechlorination.[13,14] For example, the dichloroacetamide safener dichlormid can react via abiotic reductive dechlorination to yield a previously used chloroacetamide herbicide, allidochlor (CDAA),[13] that is now banned in the United States.

There remains surprisingly little information in the peer-reviewed literature[11,15,16] regarding the environmental fate of dichloroacetamides. Available data for dichlormid and furilazole compiled from both industrial assessments and peer-reviewed studies suggest that they are at least as mobile as chloroacetamide herbicides in aqueous environments (K_d = 0.25−0.65 and 0.79−3.5 mL g^{-1}, respectively).[17−19] This is consistent with the recent detection of dichloroacetamide safeners in surface waters across Iowa and Illinois.[15] In the study by Woodward et al.,[15] the relative concentration of safeners correlated with the concentration of the active ingredient herbicides (i.e., acetochlor and metolachlor) and also scaled with large precipitation events, suggesting their origins from runoff.

In surface waters, a potentially important fate pathway for dichloroacetamide safeners is photolysis. Benoxacor can absorb light within the solar spectrum and should directly photolyze[11] (Figure S1 of the Supporting Information), although a recent study found benoxacor to be stable upon irradiation with visible (λ > 400 nm) light.[16] Other dichloroacetamide safeners (i.e., AD-67, dichlormid, and furilazole), although not capable of absorbing sunlight directly, contain moieties that may be susceptible to indirect or sensitized photolysis via reactions with reactive oxygen species (ROS) and triplet dissolved organic matter (^{3}DOM*).[11] Moreover, these other safeners can absorb light at $\lambda \sim$ 250 nm, suggesting that they could directly photolyze in ultraviolet (UV) disinfection systems.[11,14] In fact, a prior study exploring safener fate found that dichlormid, when irradiated at λ > 250 nm, yielded CDAA,[14] the same banned herbicide produced during abiotic reductive dechlorination of dichlormid.[13]

This work examines the phototransformation of dichloroacetamide safeners, aiming to quantify rates of direct and indirect photolysis and identify major photoproducts. We conducted photolysis experiments in both idealized (i.e., buffered and free of photosensitizers) and real aquatic matrices under conditions simulating sunlight and drinking water disinfection with UV light (λ > 250 nm). Photoproduct formation was initially monitored using high-performance liquid chromatography with diode array detection (HPLC−DAD) and subsequently characterized via nuclear magnetic resonance (NMR) spectroscopy and high-resolution mass spectrometry (HRMS) after isolation via liquid−liquid extraction and/or semi-preparative HPLC. Because of its ability to undergo direct photolysis, the majority of our results and product identification pertain to benoxacor. For furilazole, AD-67, and dichlormid, we report more limited results pertaining to their indirect photolysis [via ROS and possible reactive nitrogen species (RNS)] and direct photolysis under UV light. Insights produced herein should help to better predict the persistence and risk associated with safeners in agriculturally impacted surface waters.

MATERIALS AND METHODS

Reagents. Benoxacor, AD-67, furilazole, and dichlormid were purchased from commercial sources and used as received. A complete list of all reagents is available in the Supporting Information.

Photolysis Experiments. Full experimental details are presented in the Supporting Information. Most direct photolysis experiments were conducted using a commercially available 1000 W Newport Xe arc lamp with an AM 1.5 filter, a recirculated water filter to remove infrared (IR) radiation, and a 305 nm long-pass filter (lamp output over 300−400 nm = 8.8 × 10^{-3} W/cm^2; Figure S2a of the Supporting Information). Experiments were conducted in either (i) 5 mM potassium phosphate buffer adjusted to pH 5, 7, or 9, (ii) filtered (25 μm Whatman filter paper) Iowa River water, or (iii) acetonitrile at an initial safener concentration of 10 μM (corresponding to 2.1−2.8 mg/L). Additional experiments with benoxacor were conducted at a lower concentration (500 μg/L or 1.9 μM) to ensure that observed reactivity and product formation were independent of the initial safener concentration. To calculate the quantum yield (Φ), we used the *para*-nitroanisole (PNA)/pyridine actinometer system.[20−22] In all cases, aliquots of reaction mixtures (500 μL) were periodically drawn and monitored via HPLC−DAD to track reaction progress. All photolysis experiments were conducted in at least duplicate (i.e., separate experiments performed under identical conditions but conducted on different days).

A subset of direct photolysis experiments used a 200 W Newport Hg(Xe) arc lamp equipped with a 250 nm cut-on filter to simulate drinking water UV disinfection systems (output over 250−400 nm = 1.7 × 10^{-2} W/cm^2; Figure S2b of the Supporting Information). All other conditions and procedures were identical to those described for simulated sunlight experiments.

Indirect photolysis experiments were conducted using a SUNTEST CPS+ solar simulator with an irradiance setting of 750 W/m^2 and an Atlas UV SUNTEST filter to simulate wavelengths of light in the solar spectrum available on the surface of Earth (Atlas Material Testing Technology, Mount Prospect, IL, U.S.A.). An example of the irradiance spectrum is provided in Figure S2c of the Supporting Information with output over 300−400 nm of 1.3 × 10^{-2} W cm^{-2}. Reaction matrices were the same as those for direct photolysis experiments, except for the addition of photosensitizers, including 10 mg/L sodium nitrate for production of hydroxyl radical ($^\bullet$OH),[20,23,24] 10 mg/L sodium nitrite for production of $^\bullet$OH and other N-containing radicals (e.g., NO$^\bullet$),[20,23] and 10 mg/L humic acid [either Suwanee River Humic Acid (SRHA, Hamilton County, FL, U.S.A.) or Pahokee Peat Humic Acid (PPHA, Palm Beach County, FL, U.S.A.), acquired from the International Humic Substances Society] for production of ROS, such as $^\bullet$OH and singlet oxygen ($^1O_2$), and triplet-state dissolved organic matter (^{3}DOM*).[20,25] To investigate the nature of ROS in each system, some experiments were conducted with selective ROS quenchers, including isopropyl alcohol for $^\bullet$OH and sodium azide for $^1O_2$, as detailed in the Supporting Information and our prior work.[26]

Photoproduct Identification. For photoproduct identification, which was primarily explored for benoxacor, experimental systems were scaled up in safener mass and overall volume (up to ∼50 mg/L of safener in up to 1 L). Solutions were irradiated in a 1 L borosilicate glass beaker

DOI: 10.1021/acs.est.9b00861
Environ. Sci. Technol. 2019, 53, 6738−6746

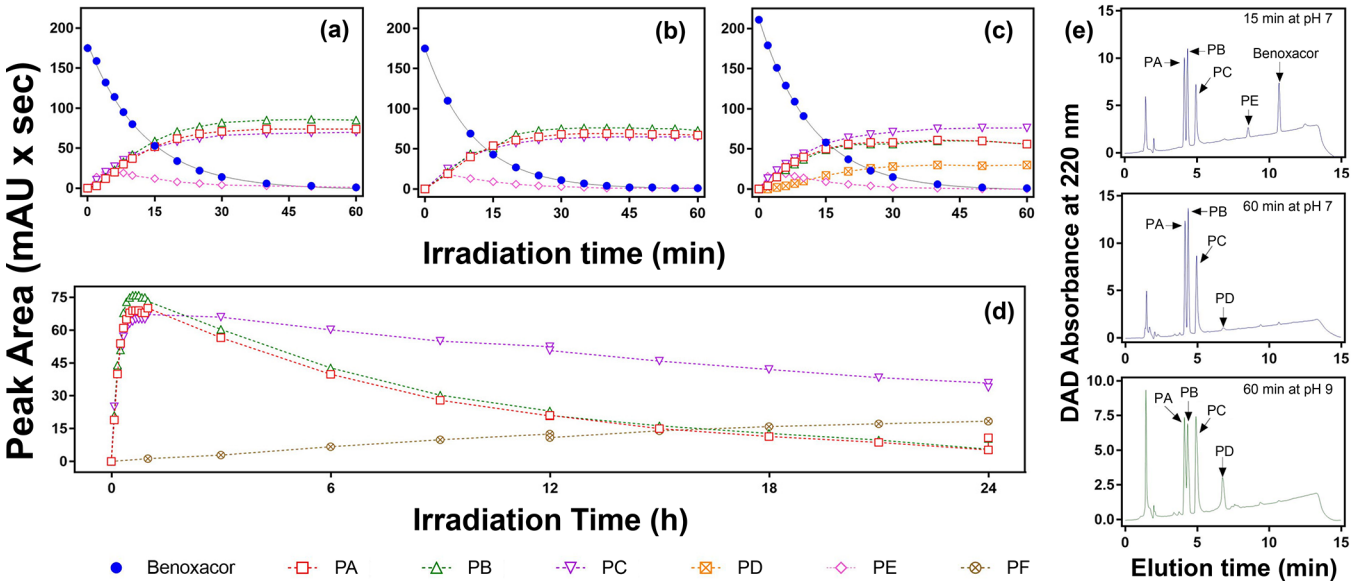

Figure 1. Direct photolysis of benoxacor at pH (a) 5, (b) 7, and (c) 9 and (d) after extended (24 h) irradiation at pH 7. (e) HPLC−DAD traces of benoxacor reaction mixtures for samples collected at the irradiation time and pH indicated. Retention times for each species are PA = 4.1 min, PB = 4.3 min, PC = 4.9 min, PD = 6.8 min, PE = 8.5 min, and benoxacor = 10.7 min. Experiments used a 1000 W Xe lamp ($\lambda \geq 305$ nm; AM 1.5 filter), and all compound peak areas were measured at a detection wavelength of 220 nm via HPLC−DAD. In time courses, solid lines represent exponential decay model fit to benoxacor data, while dashed lines simply connect data points showing concentration profiles for photoproducts. Representative data from a single experimental trial are shown, with triplicate results presented in Figures S3 and S6 of the Supporting Information.

using either the Atlas SUNTEST CPS+ solar simulator at an irradiance setting of 750 W/m^2 or the 200 W Newport Hg(Xe) arc lamp with a 250 nm long-pass, cut-on filter. Notably, direct photolysis of benoxacor at lower wavelengths (>250 nm) did not change the distribution or yields of products relative to those observed under simulated sunlight or those observed at lower initial benoxacor concentrations (10 μM). Only the rate of photoreaction increased, which proved helpful in photolyzing to completion scaled-up benoxacor systems. Reaction progress was monitored via HPLC−DAD until products reached an asymptotic level (~1.5−12 h). Upon reaction completion, samples were extracted into chloroform and concentrated to an oil/residue with compressed air. The crude reaction residues were reconstituted as highly concentrated solutions in acetonitrile (~10−20 mg of crude residue in 5−7 mL), and the components were immediately isolated via HPLC−DAD analysis and semi-preparative column fractionation.

Analytical Methods. Methods generally followed those developed by Pflug et al.[27] and are described in detail in the Supporting Information. Reactions were monitored at 220 nm and analyzed with an Agilent 1260 HPLC−DAD system equipped with a Zorbax Eclipse XDB-C_{18} column (4.6 × 150 mm, 3.5 μm) and using an acetonitrile and water gradient elution (Table S2 of the Supporting Information). Product solutions were separated on a Beckman System Gold instrument with a 166P VWD connected to a 128P solvent module using an acetonitrile and water gradient elution (2 mL min^{-1}), a 220 nm wavelength detection, and a Restek Ultra C_8 semi-preparative column (10 × 250 mm, 5 μm). For product analysis, HRMS data were gathered after either liquid chromatography (LC) or gas chromatography (GC) separation of product mixtures and via direct injection of isolated products, according to procedures in the Supporting Information. Product structures were elucidated via ^{1}H NMR, heteronuclear single quantum correlation (HSQC), and heteronuclear multiple bond correlation (HMBC) analyses as described in the Supporting Information and earlier work.[28]

RESULTS AND DISCUSSION

Benoxacor Direct Photolysis: Rate, Quantum Yield, and Trends in Photoproduct Formation. Benoxacor was the only dichloroacetamide safener found to undergo direct photolysis under simulated sunlight ($\lambda > 305$ nm). Benoxacor photolyzed rapidly following exponential (i.e., first-order) decay [average with one standard deviation of k_{obs} = 0.091 (±0.012) min^{-1}; $t_{1/2}$ ~ 8 min at pH 7; replicate data sets shown in Figure S3 of the Supporting Information] and yielded four (pH 5 and 7) or five (pH 9) major photoproducts (Figure 1), along with several minor products (data not shown). Because extinction coefficients for the photoproducts are not known, our categorization of major and minor products is simply based on relative DAD absorbance at 220 nm. We assume that product mass scales with light absorbance and that all photoproducts exhibit comparable extinction coefficients to one another and the starting material at this wavelength. Thus, the relative yields of our reported photoproducts may be slightly higher (or lower) than estimated herein if the extinction coefficient of a product at 220 nm is significantly different from that of the other species. Although product yields varied with pH, the rate constant for benoxacor decay was statistically equivalent across pH 5 [k_{obs} = 0.079 (±0.012)], 7 [k_{obs} = 0.091 (±0.012)], and 9 [k_{obs} = 0.082 (±0.013)]. We calculated an average quantum yield for benoxacor photolysis of Φ_{avg} = 0.14 (Figure S4 of the Supporting Information), suggesting a relatively efficient photoreaction.

Trends in photoproduct formation are shown in Figure 2, which presents the absorbance of each product (at 220 nm) normalized to the initial absorbance of benoxacor (also at 220 nm) as a function of reaction progress. For the x axis in Figure

DOI: 10.1021/acs.est.9b00861
Environ. Sci. Technol. 2019, 53, 6738−6746

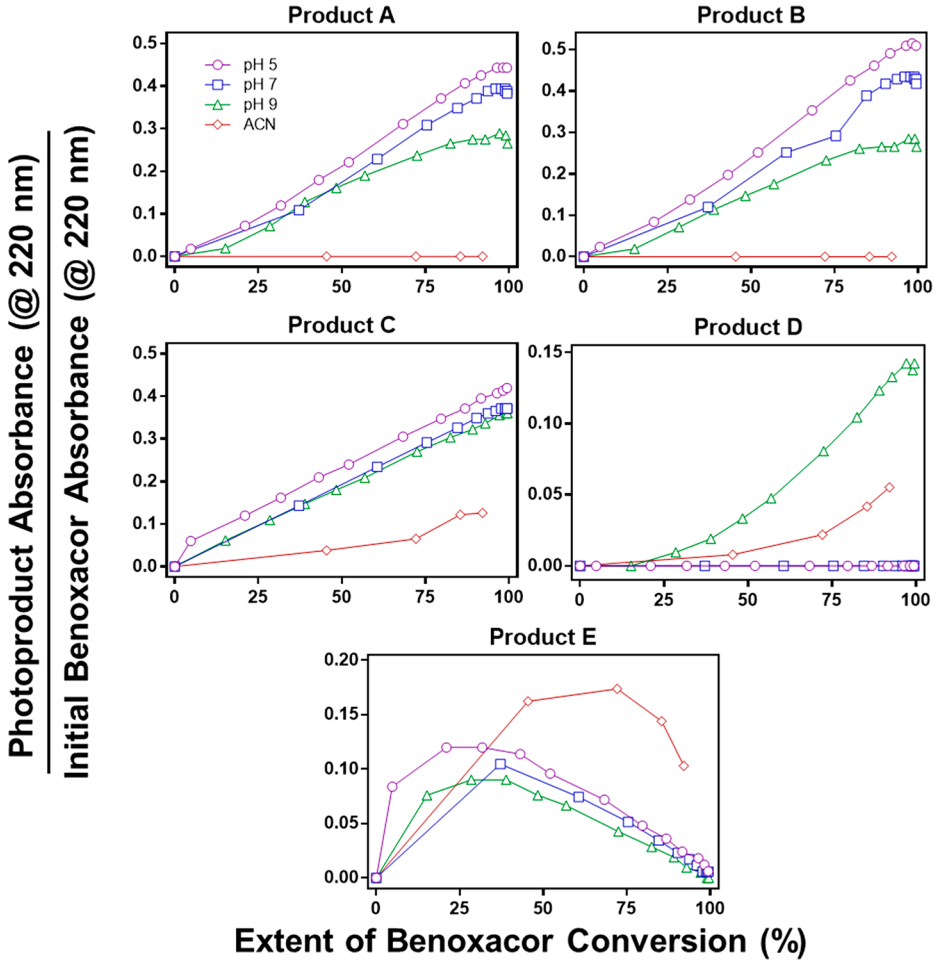

Figure 2. Benoxacor conversion to photoproducts in phosphate-buffered aqueous solutions at pH 5, 7, 9, and in acetonitrile (ACN). Plots show the peak area response for all products (A–E as measured by absorbance at 220 nm) after normalization to the initial peak area of benoxacor (also measured by absorbance at 220 nm) as a function of reaction progress (expressed as the percent of benoxacor conversion). Data are shown for pH 5 (purple circles), pH 7 (blue squares), and pH 9 (green triangles) as well as the reaction when conducted in acetonitrile (red diamonds).

2, reaction progress is expressed as the percent conversion of benoxacor as a result of direct photolysis, calculated from the percent difference of the initial concentration (measured at t = 0 before irradiation) and the measured concentration of benoxacor left in the reactor at each subsequent sampling point. When linear, the slopes of data in these plots represent an empirical estimate of photoproduct relative yields,[29] whereas a slope that is increasing or decreasing with reaction progress indicates net production or consumption, respectively, of a product. At pH 5 and 7, we assigned the following four major photoproducts denoted as products A, B, C, and E (or PA, PB, PC, and PE, respectively) based on relative elution time. In pH 9 model buffer systems and Iowa River water (pH ~ 8.5; Figure S5 of the Supporting Information), a fifth major product PD was also observed.

Each major photolysis product eluted earlier than benoxacor during HPLC–DAD analysis on our C_{18} reversed-phase column, suggesting they are more polar (Figure 1e). PA and PB eluted closely to one another and were not baseline-separated during our standard HPLC–DAD method. This required that we manually integrate these peaks by interpolating a linear baseline across the entirety of the peak area of the co-eluting products and then splitting the combined peak area via a vertical line situated at the local minimum between peaks. Yields of PA, PB, and PC all decreased with increasing pH, whereas the formation of PD was enhanced in alkaline environments and exhibited a concentration profile consistent with a secondary product (Figure 2). PE exhibited the concentration profile of a reactive intermediate (Figure 2); it formed rapidly but reached a maximum concentration after ~5 min of irradiation and subsequently decayed away relatively rapidly over the next 15 min ($t_{1/2}$ ~ 10 min; see time scales for formation and decay in Figure 1). We note that a limited number of studies were also conducted with benoxacor in the presence of up to a 10-fold molar excess of metolachlor (100 μM), an active ingredient commonly co-formulated with benoxacor that is unreactive with sunlight.[30] No changes in the rate of direct photolysis or nature and yield of photoproducts were observed in these mixtures (Figure S3 of the Supporting Information).

Benoxacor Direct Photolysis: Transformation Pathway and Photoproduct Stability. A subset of experiments was conducted in either the absence of oxygen (via N_2 sparging) or acetonitrile, a non-aqueous solvent, to explore the role of oxygen and water, respectively, in benoxacor photolysis and photoproduct formation. In the absence of oxygen, photoproduct formation trends (Figure S6 of the Supporting Information) closely matched those shown in Figure 2. However, notable differences were observed in acetonitrile; PA and PB were not produced at appreciable

DOI: 10.1021/acs.est.9b00861
Environ. Sci. Technol. 2019, 53, 6738–6746

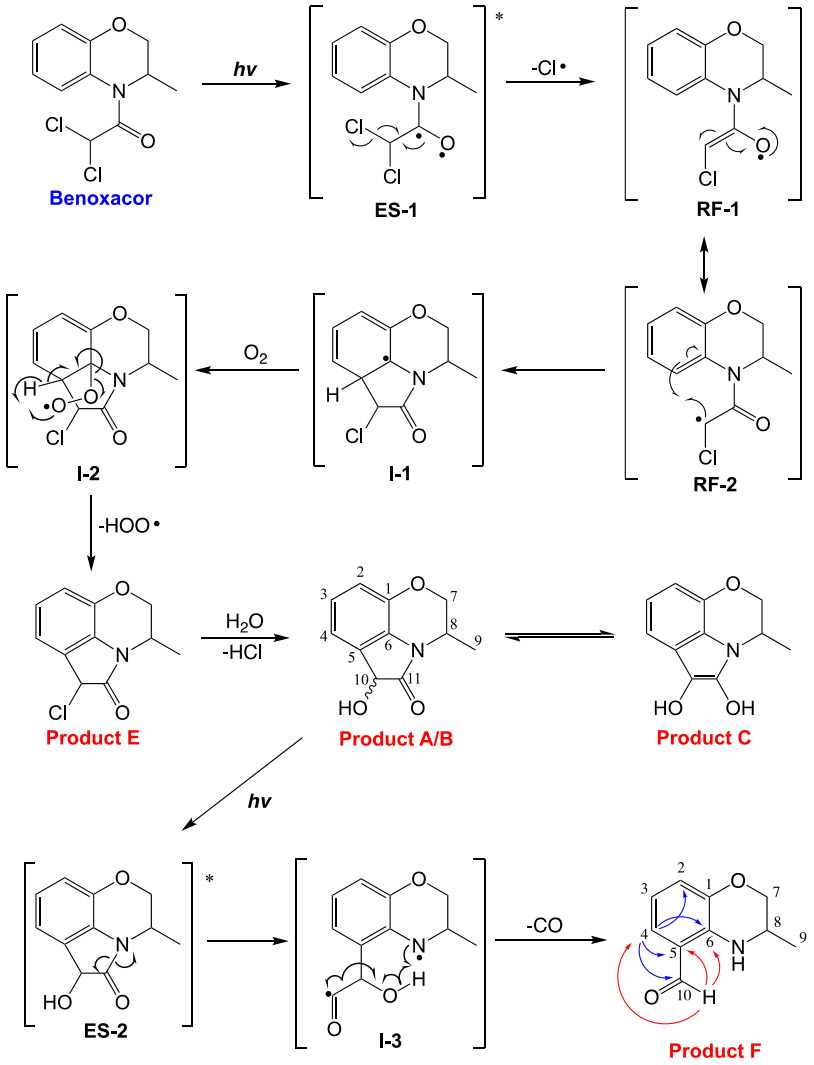

Figure 3. Proposed reaction mechanism and product formation resulting from the direct photolysis of benoxacor under simulated sunlight. Also shown are key HMBC correlations (red and blue arrows) for benoxacor photolysis product F.

quantities, while PE accumulated to a greater extent but was still reactive. Formation of PD was also enhanced in acetonitrile relative to pH 5 and 7 aqueous systems but was produced to a lesser extent than that observed in pH 9 aqueous systems.

To assess the possibility that PE may be an intermediate to the formation of other species, including PA and PB, we photolyzed benoxacor in acetonitrile for 1 h, after which aliquots of the photoproduct mixture (including some residual benoxacor) were diluted into aqueous buffer solutions (pH 5, 7, and 9). These solutions were then either stored in the absence of light to assess photoproduct thermal stability in water or photolyzed for an additional hour. In the dark, PC, PD, and PE were stable (Figure S7 of the Supporting Information), but with additional photolysis, PE quickly decayed and formation of PA and PB was observed. While this behavior is consistent with PE serving as a photoreactive intermediate to PA and PB, we cannot entirely rule out that PA and PB were generated via an alternative route directly from residual benoxacor present in the acetonitrile mixtures.

During HPLC–DAD analysis, we also noted PA and PB both exhibited local absorbance maximums at 305 nm and PC weakly absorbed at 300 nm (Figure S8 of the Supporting Information), indicating that all three could be photoactive within the solar spectrum over longer time scales. To investigate, 10 μM solutions of benoxacor were photolyzed over two complete cycles of 12 h of light (1000 W Xe arc lamp), followed by 12 h of dark to mimic diurnal cycling over multiple days in surface waters. Because all photoproducts were stable in the dark, we only present results as a function of total irradiation time (24 h) in Figure 1d.

Across 24 h of irradiation, PA, PB, and PC all decreased in concentration ($t_{1/2}$ ~6 h for PA and PB and ~24 h for PC), while a sixth major product, product F (PF), began to accumulate (Figure 1d; several more polar and less abundant products were also observed). Notably, PF was less polar (more hydrophobic) than other major products, eluting several minutes later on our reverse-phase C_{18} column (retention time of 9.4 min). Although PF accumulated over these irradiation time scales, it also can absorb light within the solar spectrum (Figure S8 of the Supporting Information) and, thus, may continue to photodegrade over even longer periods of irradiation.

Benoxacor Photoproduct Identification. *Product E.* LC–HRMS analysis of reaction mixtures after 5 min of photolysis, where PE achieves its maximum abundance, yielded

DOI: 10.1021/acs.est.9b00861
Environ. Sci. Technol. 2019, 53, 6738–6746

no observable products. We suspect PE ionized poorly during LC−HRMS analysis because a 10 μM benoxacor standard also ionized poorly using the same method. Because PE ostensibly accumulates to greater concentrations in acetonitrile (see Figure 2), we conducted complementary analysis of samples generated in acetonitrile at an initial benoxacor concentration of 500 μM, with mixture separation via either LC or GC prior to HRMS analysis. Although LC−HRMS once again yielded no observable products, GC−HRMS revealed one product with a greater abundance relative to other detectable products with a parent $M^{+\bullet}$ m/z value of 223.0399 (Figure S9 of the Supporting Information). Although directly correlating products observed via HPLC−DAD with those identified via GC−HRMS is difficult, we suspect this to be PE, the major product observable in acetonitrile.

From GC−HRMS results, PE appears to be a monochlorinated compound because of the characteristic chlorine isotope peak observed at m/z 225.0375. The mass of PE relative to benoxacor suggests its formation via loss of one chlorine atom and one hydrogen atom. We therefore propose PE to be a monochlorinated byproduct formed via a photoinitiated ring closure reaction (Figure 3), drawing analogy to proposed mechanisms for UV direct photolysis of acetochlor and metolachlor.[30,31] We speculate that a photochemical triplet π/π^* diradical excited state of benoxacor (ES-1 in Figure 3) undergoes loss of a chlorine radical to form stabilized amide enoloxy and α-amide radical resonance forms 1 and 2 (RF-1 and RF-2 in Figure 3, respectively). RF-2 would be prone to cyclization via radical addition to the benzene π system, forming a radical intermediate 1 (I-1 in Figure 3). In oxygen-containing systems, I-1 would then be susceptible to reaction with ground-state triplet molecular oxygen and the resulting peroxy radical intermediate (I-2) would be prone to hydrogen atom abstraction and the loss of hydroperoxyl to restore aromaticity, thus forming PE. Alternatively, I-1 could undergo hydrogen atom abstraction by chlorine radical and form PE directly, which would explain the same product distributions and yields observed in the absence of oxygen.

Products A, B, and C. Evidence discussed above supports PA, PB, and PC being generated from the subsequent reaction of primary photoproduct PE. PA, PB, and PC were detectable via LC−HRMS. PA had a parent ion mass $(M + H)^+$ at m/z 206.0779 with a $(M + Na)^+$ adduct at m/z 228.0601 and a $(M + K)^+$ adduct at m/z 244.0344 (Figure S10 of the Supporting Information; similar results were observed for PB and PC). Isotopic signatures were not suggestive of a chlorine substituent in PA (nor PB or PC, i.e., no chlorine-37 isotope peak at m/z ∼208).

The $(M + H)^+$ ion at m/z 206.0779 corresponds to a product with the formula $C_{11}H_{11}NO_3$, indicative of the gain of an oxygen atom and loss of two chlorine atoms from parent benoxacor. ^{1}H NMR analysis of isolated PA (Figure S11 and Table S3 of the Supporting Information) showed three aromatic proton signals with a 1,2,3-trisubstituted splitting pattern, a one-proton deshielded methine singlet at δ 4.99 (H-10), and a broad one-proton singlet at δ 4.14 (O−H). The NMR shift data for H_2-7, H-8, and H_3-9 indicated that this part of the structure (i.e., the morpholine unit) matched that of the parent compound benoxacor. ^{1}H NMR analysis of isolated PB (Figure S11 and Table S3 of the Supporting Information) showed similar signals to that observed for PA, with the exception of minor shifts in H_2-7, H-8, and H_3-9. These results are consistent with the structures proposed in Figure 3 for the two products, C-10 hydroxyl diastereomers, hence, their similar elution times on our C_{18} HPLC−DAD column. In addition, the UV spectra of the diastereomers (Figure S8 of the Supporting Information) are consistent with that of the analogous indole, 3-hydroxyindolin-2-one.[32] ^{1}H NMR analysis of isolated PC (Figure S12 and Table S4 of the Supporting Information) showed three aromatic proton signals with a 1,2,3-trisubstituted splitting pattern and two broad one-proton singlets at δ 6.81 and 6.91 (O−H). The NMR shift data for H_2-7, H-8, and H_3-9 indicated that the morpholine unit matched that of the parent compound benoxacor. Taken together, these results are consistent with PC being a tautomer (or mixture of enantiomeric tautomers) of PA and PB (Figure 3). Additionally, the UV spectrum of PC (Figure S8 of the Supporting Information) is consistent with that of the analogous indole, 2,3-dihydroxyindole.[33]

The three most abundant benoxacor photoproducts after 1 h of photolysis appear to be fully dechlorinated diastereomers (PA and PB) and their tautomer (PC) (Figure 3). The chlorine substituent of PE is expected to be susceptible to substitution involving water (or hydroxide, noting that PE accumulates to a lesser extent at pH 9 than pH 5), which would result in the loss of HCl (or chloride in alkaline conditions) and generation of the diastereomers. Because PE was stable in water in the absence of light, this substitution reaction appears to be photoassisted, even though such photosubstitutions are typically observed for aromatic substituents.[34−36] Similarly, because no interconversion of PA and PB with PC was observed in the absence of light, we also presume that tautomerization[37] is driven by light (i.e., photoenolization).[38] We posit that the small amounts of PC generated in acetonitrile systems are attributable to residual water present in the solvent, which was used as received and open to moisture from the atmosphere. On the basis of reported partitioning experiments,[39] as much as ∼10−20 mM water would likely be present in these experimental systems.

Product F. HRMS analysis of isolated PF (Figure S13 of the Supporting Information) revealed a parent ion $(M + H)^+$ at m/z 178.0859 corresponding to a product with the formula $C_{10}H_{11}NO_2$, indicative of the loss of one carbon atom and two chlorine atoms from parent benoxacor. ^{1}H NMR analysis (Figure S14 and Table S5 of the Supporting Information) indicated three aromatic proton signals with a 1,2,3-trisubstituted splitting pattern and a one-proton singlet at δ 9.83. The downfield shift of the latter suggested an aldehyde moiety, which was later confirmed by HSQC correlations (Figure S15 of the Supporting Information) from the aldehyde proton (H-10) to a carbon at δ 194.2 (C-10). As shown in Figure 3, the HMBC spectrum (Figure S16 of the Supporting Information) showed key correlations from aromatic H-4 to C-2, C-5, C-6, and aldehyde C-10 (blue arrows). Aldehyde H-10 showed key correlations to aromatic C-4, C-5, and C-6 (red arrows), thereby establishing connection of the aldehyde carbon directly to the aromatic ring at a position *ortho* to the nitrogen substituent and aromatic H-4. H_3-9 showed correlations to C-7 and C-8, which, together with the NMR shift data, indicated that the morpholine unit matched that of benoxacor, thereby allowing for the complete structural assignment of PF.

We propose that diastereomers PA and PB undergo photochemical homolytic amide bond cleavage (ES-2), resulting in diradical (I-3) formation (Figure 3), consistent with their thermal stability in water in the absence of light. I-3

DOI: 10.1021/acs.est.9b00861
Environ. Sci. Technol. 2019, 53, 6738−6746

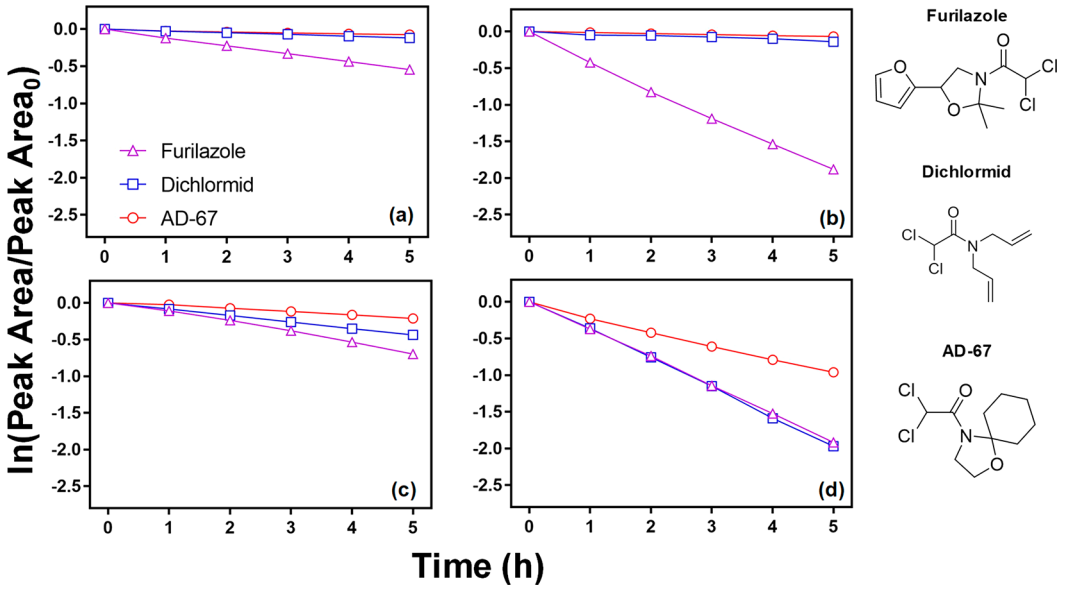

Figure 4. Semi-log plots of concentration versus time for AD-67, dichlormid, and furilazole under a SUNTEST CPS+ (750 W/m^2) in the presence of (a) 5 mg L^{-1} SRHA, (b) 10 mg L^{-1} PPHA, (c) 10 mg L^{-1} (as N) NO_3^-, and (d) 10 mg L^{-1} (as N) NO_2^-.

could then undergo an intramolecular [1,5] hydrogen shift, with subsequent loss of carbon monoxide to yield PF.

Product D. Although attempts to isolate PD were unsuccessful, we speculate that it may be formed from the dimerization of two of the PA, PB, or PC products. This is suggested by LC−HRMS analysis of the photoproduct mixture, which showed a product peak with parent ion $(M + H)^+$ of m/z 447.0938 at the same relative retention time as PD from our HPLC−DAD analysis (Figure S17 of the Supporting Information). Consistent with proposed PA, PB, or PC dimerization, there was no evidence of a chlorine substituent in the PD structure (i.e., no chlorine-37 isotope peak at m/z ~449). The formation of this dimer is unlikely to be environmentally relevant and may result from the relatively high concentration of benoxacor used to facilitate product analysis. Experiments conducted at lower benoxacor concentrations (500 μg/L) generally matched higher concentration experiments but were only conducted at pH 7, where PD is not observed.

Indirect Photolysis of AD-67, Dichlormid, and Furilazole. Because of its rapid direct photolysis, indirect photolysis of benoxacor was not investigated. For the other dichloroacetamide safeners in the presence of either 5 mg/L SRHA or 10 mg/L PPHA, only furilazole exhibited noticeable decay, with ~25 and ~80% decrease in concentration, respectively, over 5 h (panels a and b of Figure 4), accompanied by the formation of one observable, more polar transformation product. We attribute the greater reactivity of furilazole to its furan moiety, which is known to be highly reactive with singlet oxygen ($^1O_2$), one of the major ROS produced via irradiation of humic acid.[25,40] For example, it is known that furfuryl alcohol reacts with $^1O_2$ to yield various furan ring-oxidized products.[40] The addition of azide, commonly used as an $^1O_2$ quencher,[26,41] resulted in the inhibition of some but not all of the furilazole decay observed in humic acid systems (Figure S18 of the Supporting Information), which suggests that other ROS or excited-state species (e.g., triplet DOM) may contribute to transformation.

Photolysis in the presence of nitrate yields hydroxyl radical ($^\bullet$OH),[24] which resulted in the decay of all three safeners (Figure 4c). Once again, furilazole exhibited the greatest decay over 5 h (~30%), followed by dichlormid (~20%) and AD-67 (~10%). The addition of isopropyl alcohol (IPA) as a radical inhibitor entirely quenched these reactions (Figure S18 of the Supporting Information). On the basis of identical HPLC−DAD retention times and absorbance spectrum (with λ_{max} at 218 nm) (Figure S19 of the Supporting Information), it appears that the same furilazole photooxidation product is observed in nitrate systems as with humic acid. No additional products were observed for furilazole, and no transformation products were detectable via HPLC−DAD for dichlormid or AD-67.

Photolysis in the presence of nitrite (NO_2^-) also resulted in the decay of all three safeners over 5 h (Figure 4d), with more extensive transformation than observed in nitrate systems. Dichlormid and furilazole were most reactive, with nearly identical extents of decay (~80−90%) over 5 h (Figure 4d) and both yielding one detectable phototransformation product (Figures S19 and S20 of the Supporting Information). Once again, on the basis of an identical retention time and UV/vis spectra, the furilazole product appears to be identical to that observed in humic acid and nitrate systems. While nitrite photolysis results in the production of many ROS, the primary species tend to be $^\bullet$OH and NO$^\bullet$,[20,23] and use of IPA as a radical quencher completely inhibited reaction (Figure S18 of the Supporting Information). Thus, increases in the rate and extent of decay for all three safeners relative to the nitrate system may be due to RNS, such as NO$^\bullet$, which are less abundant in the nitrate system,[20,23] or greater formation of $^\bullet$OH in nitrite systems. For furilazole, the likely presence of $^\bullet$OH in nitrite systems could explain the shared transformation product observed in both nitrate and nitrite systems. This would also suggest that the furilazole product detected in humic acid systems may also be the result of reaction with $^\bullet$OH. We attribute the lower activity of AD-67 (~40% decay) relative to furilazole and dichlormid to its higher degree of

DOI: 10.1021/acs.est.9b00861
Environ. Sci. Technol. 2019, 53, 6738−6746

bond saturation, which generally would be expected to make it less reactive toward photooxidants.

Attempts to further characterize the nature of transformation products generated in humic acid, nitrate, or nitrite systems were unsuccessful. Application of LC−HRMS and GC−HRMS methods developed for benoxacor photoproduct identification failed to yield useful information as a result of either matrix complexity (e.g., humic acid systems), the relatively small extent of product formation in most mixtures, and/or the use of methods insufficiently sensitive toward these product structures.

Direct Photolysis of AD-67, Dichlormid, and Furilazole with UV Light. After over 2 h of irradiation from a 200 W lamp equipped with a 250 nm cut-on filter, AD-67, dichlormid, and furilazole directly photolyzed at nearly identical rates. Assuming exponential decay, half-lives for AD-67, dichlormid, and furilazole during UVC photolysis were all on the order of 1 h (Figure S21 of the Supporting Information). Photolysis transformation products were detected via HPLC−DAD for all three compounds while monitoring at 220 nm, but attempts to further elucidate their identify or structure were, for the most part, unsuccessful (e.g., none were readily detectable by LC−HRMS and GC−HRMS). Three transformation products were observed during UV photolysis of dichlormid. Analysis of *N*,*N*-diallyl-2-chloroacetamide (CDAA) and diallylamine reference standards via HPLC−DAD confirmed their formation via retention time matching, in agreement with the pathway proposed by Abu-Qare and Duncan (Figure S22 of the Supporting Information).[14]

■ ENVIRONMENTAL IMPLICATIONS

Herein, we established the conditions under which four widely used dichloroacetamide safeners, AD-67, benoxacor, dichlormid, and furilazole, undergo photolysis in both natural and engineered aquatic systems. Contrary to a recent investigation that only employed visible light (λ > 400 nm),[16] benoxacor rapidly photolyzes ($t_{1/2}$ ∼ 10 min) under the full spectrum of available sunlight to yield previously unreported monochlorinated and fully dechlorinated transformation products. The other dichloroacetamide safeners are more persistent, either degrading over much longer time scales through indirect pathways mediated by NOM, nitrate, and nitrite or requiring higher energy UV light only encountered in advanced water treatment systems for phototransformation.

The reactivity of benoxacor, which is among the most widely used safeners, suggests that greater attention should be paid to the occurrence, fate, and effects of its phototransformation products. Although its monochlorinated intermediate PE is relatively short-lived in sunlit aquatic systems, transport out of the photic zone could result in greater persistence as a result of its thermal stability and it may exhibit a different toxicological profile for aquatic organisms relative to benoxacor. Further, the fully dechlorinated benoxacor photoproducts (i.e., PA, PB, and PC), including the more persistent, benzaldehyde-containing PF, have not previously been reported. With recent detection of benoxacor in agriculturally impacted surface waters of the Midwest,[15] the co-occurrence of these photoproducts is likely and, if confirmed, should merit greater scrutiny of their environmental fate and mixture ecotoxicity.

Despite a recent uptick in interest of dichloroacetamide safeners from the scientific community, several knowledge gaps remain regarding their occurrence, fate, and effects. Limited work suggests their relatively high mobility in the environment, such that uptake on soil and volatilization are, at best, minor sinks for dichloroacetamide safeners in the environment.[11] Here, while we have provided a detailed evaluation of benoxacor direct photolysis, the more limited photoactivity of dichlormid, AD-67, and furilazole suggests longer persistence in surface waters unless their rate of transformation or loss via other pathways is greater. Future work should aim to identify other relevant fate pathways, establish spatial and temporal occurrence trends, and elucidate the ecotoxicity of safeners and their transformation products.

■ ASSOCIATED CONTENT

Supporting Information

The Supporting Information is available free of charge on the ACS Publications website at DOI: 10.1021/acs.est.9b00861.

Additional experimental details and results from photolysis studies and product characterization (PDF)

■ AUTHOR INFORMATION

Corresponding Author

*Telephone: 319-335-1401. E-mail: david-cwiertny@uiowa.edu.

ORCID

Nicholas C. Pflug: 0000-0002-2023-2162
Gregory H. LeFevre: 0000-0002-7746-0297
David M. Cwiertny: 0000-0001-6161-731X

Author Contributions

†Andrew E. Kral and Nicholas C. Pflug contributed equally to this work.

Notes

The authors declare no competing financial interest.

■ ACKNOWLEDGMENTS

Support for this work from the National Science Foundation (NSF) through CBET-1703796, CBET-1702610, CBET-1335711, and CHE-1609791 is gratefully acknowledged. Additional support for Monica E. McFadden was provided by a National Research Traineeship (NRT) grant from NSF (DGE-1633098). The authors thank Dr. Lynn Teesch and Vic Parcell of the University of Iowa High Resolution Mass Spectrometry Facility for their support in product analysis. The authors also thank Professor Kristopher McNeill of ETH Zurich and Professor Keith P. Reber of Towson University for fruitful mechanistic discussions as well as the helpful comments of three anonymous reviewers whose feedback improved the clarity and quality of this work.

■ REFERENCES

(1) Cobb, A.; Reade, J. *Herbicides and Plant Physiology*, 2nd ed.; Wiley-Blackwell: West Sussex, U.K., 2010; p 286.

(2) Davies, J.; Caseley, J. Herbicide safeners: A review. *Pestic. Sci.* **1999**, *55*, 1043−1058.

(3) Rosinger, C. Herbicide safeners: An overview. *Julius-Kühn-Archiv.* **2014**, *443*, 516−525.

(4) Rosinger, C.; Kocher, H. Safeners for herbicides. In *Modern Crop Protection Chemicals*; Kramer, W., Schirmer, U., Eds.; John Wiley: Weinheim, Germany, 2007; pp 259−281.

(5) Schulze, E.-D.; Beck, E.; Müller-Hohenstein, K. *Plant Ecology*; Springer: Berlin, Germany, 2002.

(6) Zhang, Q.; Xu, F.; Lambert, K. N.; Riechers, D. E. Safeners coordinately induce the expression of multiple proteins and MRP

DOI: 10.1021/acs.est.9b00861
Environ. Sci. Technol. 2019, 53, 6738−6746

transcripts involved in herbicide metabolism and detoxification in *Triticum tauschii* seedling tissues. *Proteomics* **2007**, *7*, 1261−1278.
(7) Pang, S.; Duan, L.; Liu, Z.; Song, X.; Li, X.; Wang, C. Co-induction of a glutathione-*S*-transferase, a glutathione transporter and an ABC transporter in maize by xenobiotics. *PLoS One* **2012**, *7*, No. e40712.
(8) Edwards, R.; Del Buono, D.; Fordham, M.; Skipsey, M.; Brazier, M.; Dixon, D. P.; Cummins, I. Differential induction of glutathione transferases and glucosyltransferases in wheat, maize and *Arabidopsis thaliana* by herbicide safeners. *Z. Naturforsch., C: J. Biosci.* **2005**, *60*, 307−316.
(9) United States Government. Federal Insecticide, Fungicide, and Rodenticide Act (FIFRA). In *Code of Federal Regulations (CFR)*; Government Printing Office: Washington, D.C., 2012, Vol. 7, U.S.C. 136-136y.
(10) United States Environmental Protection Agency (U.S. EPA). Benoxacor Pesticide Tolerances, Final Rule. *Fed. Regist.* **1998**, *63*, 7299−7305.
(11) Sivey, J. D.; Lehmler, H.-J.; Salice, C. J.; Ricko, A. N.; Cwiertny, D. M. Environmental Fate and Effects of Dichloroacetamide Herbicide Safeners: "Inert" Yet Biologically Active Agrochemical Ingredients. *Environ. Sci. Technol. Lett.* **2015**, *2*, 260−269.
(12) Bolyard, K.; Gresens, S. E.; Ricko, A. N.; Sivey, J. D.; Salice, C. J. Assessing the toxicity of the "inert" safener benoxacor toward *Chironomus riparius*: Effects of agrochemical mixtures. *Environ. Toxicol. Chem.* **2017**, *36*, 2660−2670.
(13) Sivey, J. D.; Roberts, A. L. Abiotic Reduction Reactions of Dichloroacetamide Safeners: Transformations of "Inert" Agrochemical Constituents. *Environ. Sci. Technol.* **2012**, *46*, 2187−2195.
(14) Abu-Qare, A. W.; Duncan, H. J. Photodegradation of the herbicide EPTC and the safener dichlormid, alone and in combination. *Chemosphere* **2002**, *46*, 1183−1189.
(15) Woodward, E. E.; Hladik, M. L.; Kolpin, D. W. Occurrence of Dichloroacetamide Herbicide Safeners and Co-applied Herbicides in Midwestern U.S. Streams. *Environ. Sci. Technol. Lett.* **2018**, *5*, 3−8.
(16) Acharya, S. P.; Weidhaas, J. Solubility, partitioning, oxidation and photodegradation of dichloroacetamide herbicide safeners, benoxacor and furilazole. *Chemosphere* **2018**, *211*, 1018−1024.
(17) Carr, K. H. *Adsorption/Desorption Studies of MON 13909 and Aerobic Soil Metabolites*; Monsanto Agricultural Company: Creve Coeur, MO, 1990; http://www.epa.gov/pesticides/chemicalsearch/chemical/foia/clearedreviews/reviews/911596/911596-1993-06-30i.pdf (accessed July 16, 2015).
(18) Subba-Rao, R. V. *R-25788: Adsorption and Desorption in Four Soils*; ICI Americas, Inc.: Wilmington, DE, 1990; http://www.epa.gov/pesticides/chemicalsearch/chemical/foia/cleared-reviews/reviews/900497/900497-1993-01-08e.pdf (accessed July 16, 2015).
(19) Liu, W.; Gan, J.; Papiernik, S. K.; Yates, S. R. Structural Influences in Relative Sorptivity of Chloroacetanilide Herbicides on Soil. *J. Agric. Food Chem.* **2000**, *48*, 4320−4325.
(20) Schwarzenbach, R. P.; Gschwend, P. M.; Imboden, D. M. *Environmental Organic Chemistry*, 2nd ed.; Wiley: Hoboken, NJ, 2003.
(21) Leifer, A. *The Kinetics of Environmental Aquatic Photochemistry: Theory and Practice*; American Chemical Society (ACS): Washington, D.C., 1988.
(22) Laszakovits, J. R.; Berg, S. M.; Anderson, B. G.; O'Brien, J. E.; Wammer, K. H.; Sharpless, C. M. *p*-Nitroanisole/Pyridine and *p*-Nitroacetophenone/Pyridine Actinometers Revisited: Quantum Yield in Comparison to Ferrioxalate. *Environ. Sci. Technol. Lett.* **2017**, *4*, 11−14.
(23) Mack, J.; Bolton, J. R. Photochemistry of nitrite and nitrate in aqueous solution: A review. *J. Photochem. Photobiol., A* **1999**, *128*, 1−13.
(24) Zepp, R. G.; Hoigne, J.; Bader, H. Nitrate-induced photooxidation of trace organic chemicals in water. *Environ. Sci. Technol.* **1987**, *21*, 443−450.
(25) Mostofa, K. M. G.; Liu, C.-q.; Mottaleb, M. A.; Wan, G.; Ogawa, H.; Vione, D.; Yoshioka, T.; Wu, F. Dissolved Organic Matter in Natural Waters. In *Photobiogeochemistry of Organic Matter: Principles and Practices in Water Environments*; Mostofa, K. M. G., Yoshioka, T., Mottaleb, A., Vione, D., Eds.; Springer: Berlin, Germany, 2013; pp 1−137, DOI: 10.1007/978-3-642-32223-5_1.
(26) Qu, S.; Kolodziej, E. P.; Cwiertny, D. M. Phototransformation Rates and Mechanisms for Synthetic Hormone Growth Promoters Used in Animal Agriculture. *Environ. Sci. Technol.* **2012**, *46*, 13202−13211.
(27) Pflug, N. C.; Hankard, M. K.; Berg, S.; O'Connor, M.; Gloer, J. B.; Kolodziej, E. P.; Cwiertny, D. M.; Wammer, K. H. Environmental photochemistry of dienogest: Phototransformation to estrogenic products and increased environmental persistence via reversible photohydration. *Environ. Sci.: Processes Impacts* **2017**, *19*, 1414−1426.
(28) Pflug, N. C. Identification of Bioactive Products from Environmental Transformation of Steroids. Ph.D. Thesis, Department of Chemistry, University of Iowa, Iowa City, IA, 2017.
(29) Baltrusaitis, J.; Patterson, E. V.; O'Connor, M.; Qu, S.; Kolodziej, E. P.; Cwiertny, D. M. Reversible Photohydration of Trenbolone Acetate Metabolites: Mechanistic Understanding of Product-to-Parent Reversion through Complementary Experimental and Theoretical Approaches. *Environ. Sci. Technol.* **2016**, *50*, 6753−6761.
(30) Wu, C.; Shemer, H.; Linden, K. G. Photodegradation of Metolachlor Applying UV and UV/H_2O_2. *J. Agric. Food Chem.* **2007**, *55*, 4059−4065.
(31) Souissi, Y.; Bourcier, S.; Ait-Aissa, S.; Maillot-Maréchal, E.; Bouchonnet, S.; Genty, C.; Sablier, M. Using mass spectrometry to highlight structures of degradation compounds obtained by photolysis of chloroacetamides: Case of acetochlor. *J. Chromatogr. A* **2013**, *1310*, 98−112.
(32) Sadauskas, M.; Vaitekūnas, J.; Gasparavičiūtė, R.; Meškys, R. Indole Biodegradation in *Acinetobacter* sp. Strain O153: Genetic and Biochemical Characterization. *Appl. Environ. Microbiol.* **2017**, *83*, e01453-17.
(33) Fujioka, M.; Wada, H. The bacterial oxidation of indole. *Biochim. Biophys. Acta, Gen. Subj.* **1968**, *158*, 70−78.
(34) Cornelisse, J.; De Gunst, G. P.; Havinga, E.; Gold, V. Nucleophilic Aromatic Photosubstitution. *Adv. Phys. Org. Chem.* **1975**, *11*, 225−266.
(35) Cornelisse, J.; Havinga, E. Photosubstitution reactions of aromatic compounds. *Chem. Rev.* **1975**, *75*, 353−388.
(36) Cornelisse, J.; Lodder, G.; Havinga, E. Pathways and intermediates of nucleophilic aromatic photosubstitution reactions. *Rev. Chem. Intermed.* **1979**, *2*, 231−265.
(37) Raczyńska, E. D.; Kosińska, W.; Ośmiałowski, B.; Gawinecki, R. Tautomeric Equilibria in Relation to Pi-Electron Delocalization. *Chem. Rev.* **2005**, *105*, 3561−3612.
(38) Klán, P.; Wirz, J.; Gudmundsdóttir, A. Photoenolization and Its Applications. In *CRC Handbook of Oragnic Photochemistry and Photobiology*, 3rd ed.; CRC Press (Taylor & Francis Group): Boca Raton, FL, 2012; pp 627−652.
(39) Hui, Y.; Webster, R. D. Absorption of Water into Organic Solvents Used for Electrochemistry under Conventional Operating Conditions. *Anal. Chem.* **2011**, *83*, 976−981.
(40) Gollnick, K.; Griesbeck, A. Singlet oxygen photooxygenation of furans: Isolation and reactions of (4 + 2)-cycloaddition products (unsaturated *sec*-ozonides). *Tetrahedron* **1985**, *41*, 2057−2068.
(41) Werner, J. J.; McNeill, K.; Arnold, W. A. Environmental photodegradation of mefenamic acid. *Chemosphere* **2005**, *58*, 1339−1346.

DOI: 10.1021/acs.est.9b00861
Environ. Sci. Technol. 2019, 53, 6738−6746